Biochimica et Biophysica Acta 819 (1985) 93–104
Elsevier

BBA 72710

Stoichiometric and electrostatic characterization of calcium binding to native and lipid-substituted adenosinetriphosphatase of sarcoplasmic reticulum

Helena Scofano [a], Hector Barrabin [a], Giuseppe Inesi [a] and Joel A. Cohen [b,*]

[a] *Department of Biological Chemistry, University of Maryland, Baltimore, MD, 21201 and* [b] *Department of Physiology, University of the Pacific, San Francisco, CA 94115 (U.S.A.)*

(Received January 30th, 1985)
(Revised manuscript received May 15th, 1985)

Key words: Sarcoplasmic reticulum; Lipid substitution; Ca^{2+} binding; Gouy-Chapman-Stern theory; ATPase; (Rabbit muscle)

The stoichiometry of calcium binding to specific sites (i.e., those producing enzyme activation) was found to be 8–10 nmol/mg protein in native sarcoplasmic reticulum vesicles, and 13.9–15.4 nmol/mg of ATPase purified by non-ionic detergent solubilization and anion exchange chromatography. Parallel measurements of phosphoenzyme yielded levels of 4.0–4.9 and 6.0–7.7 nmol/mg of protein in the two preparations, respectively, demonstrating that each 115 kDa ATPase chain includes one catalytic site and two calcium binding sites. The apparent association constant, $K = (6 \pm 2) \cdot 10^5$ M^{-1}, and the binding cooperativity, $n_H = 1.9$, were unchanged when measurements were carried out with native sarcoplasmic reticulum vesicles and when the membrane surface charge was altered by lipid substitution with phosphatidylcholine or phosphatidylserine, at neutral pH in the presence of 10 mM $MgCl_2$ and 80 mM KCl. On the other hand, the apparent association constant was increased in the absence of Mg^{2+} or, to a lesser extent, in the absence of monovalent cations. It was also observed that the cooperative character of the calcium binding isotherms was reduced in low ionic-strength media. Analysis of the electrostatic effects indicates that the calcium-binding domain is shielded from the membrane phospholipid surface charge by virtue of its location within the ATPase protein. The effects of various electrolytes are attributed to monovalent-cation binding in the calcium-binding domain. The apparent loss of cooperativity of the calcium binding isotherms at low ionic strength is attributed to a progressive displacement of the titration curve which is minimal at low degrees of saturation and becomes larger at higher degrees of saturation. This behavior is described quantitatively by the progressive effect of calcium binding on an electrostatic potential generated by localized protein charge densities within, or near, the calcium-binding domain.

Introduction

Measurements of calcium binding to sarcoplasmic reticulum vesicles following equilibration with radioactive tracer reveal two or three classes of binding sites of different affinities [1]. The high-affinity class, which is involved in enzyme activation, displays cooperative behavior and accounts for 8–10 nmoles of calcium bound per mg of protein in sarcoplasmic reticulum vesicles [2–4] and 10–12 nmol/mg of protein [5] purified by fractional solubilization with ionic detergents [6,7]. These values are less than expected (17.4 nmol/mg protein) assuming that the purified pre-

* To whom correspondence should be addressed.

Abbreviations: $C_{12}E_8$, dodecyl octaethylene glycol monoether; EGTA, ethylene glycol bis(β-aminoethyl ether)-*N*,*N*′-tetra-acetic acid; Mes, 4-morpholineethanesulfonic acid; Mops, 4-morpholinepropanesulfonic acid; PC, phosphatidylcholine; PS, phosphatidylserine; PI, phosphatidylinositol; PG, phosphatidylglycerol.

parations contain only active ATPase and that each 115 kDa ATPase chain binds two calcium ions. In order to resolve this basic question of stoichiometry, we measured calcium binding to sarcoplasmic reticulum ATPase purified by solubilization with a non-ionic detergent and anion exchange chromatography, which was recently reported to yield levels of phosphorylated enzyme intermediate corresponding to one phosphorylation (catalytic) site per 115 kDa ATPase chain [8–10]. Since this purification method permits replacement of native sarcoplasmic-reticulum lipids with phosphatidylcholine (PC) or phosphatidylserine (PS), we also studied the effect of lipid charge on calcium binding. Finally, we determined a series of calcium binding isotherms in media of different electrolyte composition and investigated the electrostatic mechanisms involved in calcium binding to the high-affinity sites of sarcoplasmic reticulum ATPase.

Experimental procedures

Sarcoplasmic reticulum vesicles were obtained from rabbit skeletal muscle as previously described [11]. Purified ATPase was prepared according to Barrabin et al. [8] as follows: a sufficient amount of preswollen DEAE (DE-52, Whatman) cellulose was suspended in 100 ml of equilibration buffer (20 mM Tris-HCl (pH 7.3), 0.1 mM $CaCl_2$, 120 mM NaCl, 20% (v/v) glycerol, and 0.5 mg dodecyl octaethylene glycol monoether ($C_{12}E_8$) per ml) to yield 35 ml of packed gel. The slurry was adjusted to pH 7.3, poured into a Bio-Rad econocolumn, and equilibrated with at least 250 ml equilibration buffer which was allowed to flow until only a minimal layer was left on top of the gel column. Meanwhile, sarcoplasmic reticulum vesicles (50 mg protein) were dissolved in 25 ml of a medium containing 20 mM Tris-HCl (pH 7.5), 0.1 mM $CaCl_2$, 50 mM NaCl, 20% (v/v) glycerol, and 4 mg $C_{12}E_8$/ml. The solubilized protein was passed through an HA 0.45 μm Millipore filter, placed on top of the gel in the chromatography column, and allowed to flow at a rate of 0.16–0.17 ml/min. Equilibration medium (approximately one-third of the column volume) was added just when the solubilization solution had entered the column, and nonspecific protein was washed out until the absorbance ($\lambda = 280$ nm) reached the baseline. The elution flow was then increased to 0.250 ml/min, and when the elution fluid had entirely entered the column, elution buffer (20 mM Tris-HCl (pH 7.3), 0.1 mM $CaCl_2$, 120 mM NaCl, 20% (v/v) glycerol, and 0.5 mg $C_{12}E_8$/ml) was added and the elution flow increased 3- or 4-fold. Drying of the gel and air bubbles were avoided at all times.

The elution peak contained ATPase which was mostly delipidated (8–10 moles of phospholipid phosphorus remaining per mole of ATPase chain) and displayed very low activity. This fraction was pooled, diluted with elution buffer to a protein concentration of 2.0–2.5 mg/ml, and exogenous phospholipid (2.0–2.5 mg/ml) was added. For this purpose an appropriate volume of a chloroform-methanol solution of phosphatidylcholine (Type V-EA, Sigma) or bovine-brain phosphatidylserine (Sigma) was dried with a stream of nitrogen, the dry residue was dispersed with elution medium to a concentration of 30 mg phospholipid/ml, and the dispersion was immersed in a sonicator bath for two minutes. The sonicated lipid was then simply added to the ATPase eluate, and the mixture was incubated for 90 min at room temperature.

When a more concentrated protein suspension was required, the glycerol contained in the suspension was removed by passing the samples through a Bio-Gel P-10 (Bio-Rad) column equilibrated with 20 mM Tris-HCl (pH 7.3), 50 mM NaCl, and 20 μM $CaCl_2$. The eluate was centrifuged for 30 min at $30\,000 \times g$, and the pellet was resuspended in a suitable volume of elution medium (without glycerol).

The entire procedure was carried out at room temperature, and the final samples were stored at -70°C after freezing with an acetone/solid CO_2 mixture.

ATPase activity was assessed by measuring P_i cleavage from ATP in media containing 20 mM Tris-HCl (pH 7.5), 0.1 mM $CaCl_2$, 80 mM KCl, 10 mM $MgCl_2$, and 10–15 μg protein/ml. When indicated, $C_{12}E_8$ (1 mg/ml) was also present. The reaction was started by the addition of 2 mM ATP and quenched with molybdovanadate reagent [12] after 1 min incubation at 37°C.

Enzyme phosphorylation with [γ-^{32}P]ATP, or

$^{32}P_i$, was measured as follows: Phosphorylation by ATP was carried out at 25°C for 10 s in a reaction medium containing 30 mM Tris-HCl buffer (pH 7.5), 5 mM $MgCl_2$, 10 mM $CaCl_2$, 80 mM KCl, and 0.1 mM [γ-^{32}P]ATP. Phosphorylation by P_i was carried out in a reaction medium containing 30 mM Mes-Tris buffer (pH 6.0), 40% Me_2SO, 20 mM $MgCl_2$, 1 mM EGTA, and 1 mM $^{32}P_i$-Tris for 10 min at 25°C. The reaction was initiated by addition of [γ-^{32}P]ATP or $^{32}P_i$ and quenched by the addition of ice-cold perchloric acid containing P_i (final concentrations 125 mM and 4 mM, respectively). The protein precipitate was washed three times with 4 ml aliquots of ice-cold 125 mM perchloric acid containing 4 mM P_i and once with 4 ml of water. The washed pellets were dissolved in 0.35 ml of 1% lithium dodecyl sulfate, 0.1 M Li_2SO_4, and 0.05 M lithium acetate (pH 4.5). Aliquots were taken for protein determination and liquid scintillation counting.

Calcium binding was determined by measuring the distribution of radioactive calcium tracer following equilibration in chromatography columns [2], and/or by measuring the calcium-induced change of protein intrinsic fluorescence [13–15,34]. For the direct measurement of binding [2], small columns (0.5 × 12.0 cm) were filled with Bio-Gel P-50 (50–100 mesh) and equilibrated with an elution medium containing buffer, radioactive calcium, and other electrolytes as specified in the legends to the figures. A concentrated suspension (1 mg) of protein was then placed on top of the column and allowed to elute. Radioactive calcium and protein concentration were then determined in fractional elution samples. The excess calcium (over the baseline) eluting with the protein peak was considered bound.

Measurements of intrinsic fluorescence were carried out with an Aminco-Bowman spectrofluorometer equipped with thermostatted cell holder (25°C) and cuvette stirrer. Excitation wavelength was 290 nm and the emission intensity was measured at 330 nm. The protein concentration was 0.1 mg/ml, and the medium contained the electrolyte compositions given in the legends to the figures. Calcium or EGTA additions were made with very small volumes, and the dilution effects on fluorescence intensity were taken into account.

Total calcium was measured by atomic absorption spectrometry or by double-wavelength photometry and titration with EGTA in the presence of the metallochromic indicator murexide. Free Ca^{2+} concentrations were estimated from total calcium and EGTA by computations [16], taking into account pH, Mg^{2+} and K^+ concentrations, and the binding constants given by Allen et al. [17].

Protein concentration in the presence of $C_{12}E_8$ and glycerol was measured by the Lowry method [18] modified according to Peterson [19].

Phospholipid phosphorus was measured by the method of Barlett [20].

Results

Binding stoichiometry

The first aim of our study was to define the stoichiometry of specific (high-affinity) calcium-binding sites and phosphorylation (catalytic) sites in sarcoplasmic reticulum ATPase purified by solubilization with a non-ionic detergent and by anion exchange chromatography [8]. Since the enzyme is largely delipidated (8–10 moles of phospholipid phosphorus remaining per mole of ATPase chain) during the chromatographic procedure, exogenous lipids and/or detergent must be added to restore ATPase activity. Relative to sarcoplasmic reticulum vesicles (rendered leaky with detergent), the purified ATPase shows an approximately 2-fold increase in hydrolytic activity when enriched with PC or PS, although the PS (but not the PC) preparation requires addition of detergent for full expression of enzymatic activity (Table I). We found that, independent of whether the purified enzyme is enriched with PC or PS, the specific calcium binding (measured at equilibrium in the presence of ^{45}Ca concentrations saturating the high-affinity sites) increases from 8.0–10.0 nmol/mg protein obtained with native sarcoplasmic reticulum vesicles, to 13.9–15.4 nmol/mg of purified protein (Table I). Concurrently, the maximal level of phosphorylated intermediate rises from 4.0–4.9 nmol/mg protein in native sarcoplasmic reticulum vesicles, to 6.0–7.7 nmol/mg of purified enzyme (Table I). Considering that 1 mg of purified enzyme contains a maximum of 8.7 nmol of 115 kDa polypeptide chains, it is apparent that the stoichiometric ratio of specific calcium

TABLE I

MAXIMAL LEVELS OF HYDROLYTIC ACTIVITY, PHOSPHORYLATED ENZYME INTERMEDIATE, AND CALCIUM BINDING IN NATIVE SARCOPLASMIC RETICULUM VESICLES AND IN PURIFIED ATPASE RELIPIDATED WITH PC OR PS

Addition of $C_{12}E_8$ was required to obtain maximal levels of hydrolytic activity (but not of phosphoenzyme or calcium binding) of only the PS-ATPase. SR, sarcoplasmic reticulum.

Preparation	Hydrolytic activity (μmol/mg min)	Phosphoenzyme (nmol/mg)	Ca^{2+} binding (nmol/mg)
SR vesicles	6.3–7.7	4.0–4.9	8.0–10.0
ATPase + PC	12.2–13.6	6.2–7.7	13.9–14.9
ATPase + PS	4.2–6.0	6.0–7.5	14.1–15.4
ATPase + PS + $C_{12}E_8$	11.2–13.6	–	–

sites to phosphorylation sites to 115 kDa polypeptide chains is 2 : 1 : 1. This ratio is identical in preparations enriched with PC or PS.

Binding isotherms of native and PC- or PS-enriched ATPase

We then proceeded to determine the Ca^{2+} concentration dependence of calcium binding in 'standard' media (10 mM $MgCl_2$, 80 mM KCl, pH 6.8) which are most commonly used in studies of enzyme activity. It is shown in Fig. 1 that the calcium binding isotherms obtained both with sarcoplasmic reticulum vesicles and with purified ATPase enriched with PC or PS are identical, displaying half-maximal saturation in the presence of 1.3 μM Ca^{2+}, and definitely cooperative (n_H = 1.9) behavior. Therefore, in 'standard' media, calcium binding to specific sites involved in activation of sarcoplasmic reticulum ATPase is not significantly influenced by the phospholipid charge of the membrane bilayer. This is in agreement with

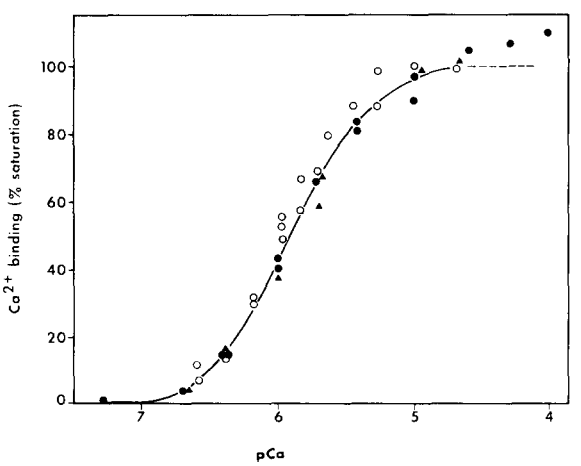

Fig. 1. Ca^{2+} concentration dependence of calcium binding to native sarcoplasmic reticulum vesicles (○) and to ATPase purified and relipidated with PC (●) or PS (▲). Calcium binding was measured directly by [^{45}Ca]Ca equilibration in chromatography columns [2] in the presence of 20 mM Mops (pH 6.8), 10 mM $MgCl_2$, 80 mM KCl, and either 40 μM $CaCl_2$ and EGTA to lower the free Ca^{2+} concentration, or Ca^{2+} (without EGTA) to yield free Ca^{2+} concentrations higher than 40 μM. The solid curve has been drawn empirically through the data points.

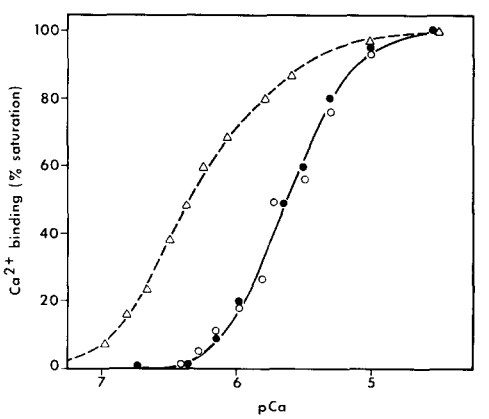

Fig. 2. Effect of K^+ and Mg^{2+} on calcium binding to native sarcoplasmic reticulum vesicles. In addition to 20 mM Mops (pH 6.8), 0.1 mM total calcium, and EGTA to yield various free Ca^{2+} concentrations, the equilibration medium contained 10 mM $MgCl_2$ and 80 mM KCl (●), 10 mM $MgCl_2$ and no KCl (○), or neither $MgCl_2$ nor KCl (△). Calcium binding was determined by measuring changes of protein intrinsic fluorescence. The titration was started by adding increasing concentrations of EGTA to 0.1 mM total Ca^{2+}. The solid curve has been drawn empirically through the data points. The dashed curve has been calculated by the Gouy-Chapman-Stern theory as described in the text.

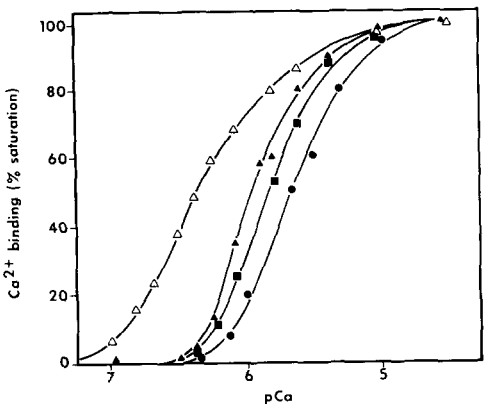

Fig. 3. Calcium binding to native sarcoplasmic reticulum vesicles in the presence of different concentrations of KCl. In addition to 20 mM Mops (pH 6.8), 0.1 mM total calcium, and EGTA to yield various free Ca^{2+} concentrations, the equilibration medium contained 80 mM KCl and 10 mM $MgCl_2$ (●), neither KCl nor $MgCl_2$ (△), 80 mM KCl and no $MgCl_2$ (▲), 200 mM KCl and no $MgCl_2$ (■). Calcium binding was determined by measuring changes of protein intrinsic fluorescence. The solid curves have been drawn empirically through the data points.

previous reports by Fiehn and Migala [21] and Medda and Hasselbach [22], who showed that calcium binding is not affected even by removal of lipid.

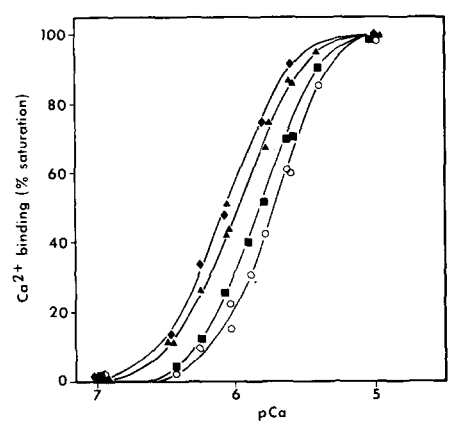

Fig. 4. Calcium binding to native sarcoplasmic reticulum vesicles in the presence of different monovalent cations. In addition to 20 mM Mops (pH 6.8), 0.1 mM total calcium, and EGTA to yield various free Ca^{2+} concentrations, the equilibration medium contained 200 mM of either CsCl (◆), choline chloride (▲), KCl (■), or LiCl (○). No Mg^{2+} was added. Calcium binding was determined by measuring changes of protein intrinsic fluorescence. The solid curves have been drawn empirically through the data points.

Effects of electrolytes on calcium binding

When we extended our experimentation to variation of the electrolyte composition of the medium, we found that omission of Mg^{2+} increased the affinity of non-specific calcium binding sites to a range that interfered with selective titration of the specific sites with radioactive tracer. We then resorted to measurements of protein intrinsic fluorescence, since it is known that this signal arises from calcium binding to specific sites, and it is not affected by calcium binding to non-specific sites of the sarcoplasmic reticulum ATPase [13–15,34].

In Figs. 2–4 we illustrate the effect of altering the electrolyte ionic strength and composition on the binding of calcium to the ATPase of native sarcoplasmic reticulum vesicles. It is shown in Fig. 2 that the calcium binding isotherm obtained in the absence of Mg^{2+} and K^+ displays a higher affinity ($K = 2.3 \cdot 10^6$ M^{-1}) and a lower cooperativity ($n_H = 1.2$–1.3) than those obtained in 'standard' (10 mM Mg^{2+} and 80 mM K^+) media ($K = 4.5 \cdot 10^5$ M^{-1}, $n_H = 1.9$). It is of interest that addition of Mg^{2+}, even in the absence of K^+, returns both affinity and cooperativity to levels identical to those observed in the presence of both K^+ and Mg^{2+} (Fig. 2). On the other hand, in the absence of Mg^{2+}, addition of K^+ up to 200 mM only partially lowers the affinity of the enzyme for Ca^{2+}, while it does restore the full cooperative character of the binding isotherm (Fig. 3). In the absence of Mg^{2+}, a comparison of the effects of Cs^+, choline$^+$, K^+, and Li^+ shows that a reduction of the enzyme affinity for Ca^{2+} is produced by these cations with a pattern related to their ionic radii (Fig. 4). On the other hand, the cooperative character of binding is fully restored by all of these monovalent cations, independent of their ionic radii. At saturating Ca^{2+} the maximal calcium bound is the same, independent of the electrolyte composition of the medium.

Discussion

Binding stoichiometry

The stoichiometry of calcium binding with respect both to the phosphorylation (catalytic) sites and to the 115 kDa polypeptide chains of the sarcoplasmic reticulum ATPase is an important issue. From the functional standpoint, this issue is

related to the pumping ratio of two moles of calcium per mole of ATP [23], and to the cooperativity of calcium binding that requires at least two interacting sites at neutral pH [2] and four interacting sites at alkaline pH [5]. In our preparations of purified ATPase we find that each 115 kDa polypeptide chain includes two calcium sites and one phosphorylation (catalytic) site. This indicates that each 115 kDa chain has the correct stoichiometry of calcium and catalytic sites to account for the stoichiometry observed experimentally in active transport. In fact some evidence indicates that sarcoplasmic reticulum ATPase is active as a catalyst and energy transducer in the monomeric state [24,25], although it cannot be excluded that actual translocation of calcium across the membrane requires oligomeric assembly of the chains. On the other hand, interaction of two chains, together comprising four calcium sites and two catalytic sites, may be required to explain the high degree of binding cooperativity observed at alkaline pH [4] as well as some features of the enzyme kinetics [26]. Such a dimeric interaction is consistent with recent observations on bidimensional crystals of sarcoplasmic reticulum ATPase [27].

Binding isotherms of native and PC- or PS-enriched ATPase

In general, as a result of membrane surface charge, the ATPase Ca^{2+} binding site may reside in a region whose electrostatic potential differs from that of the bulk solution. The aqueous Ca^{2+} concentration at the binding site, relative to that in the bulk solution, is then given by the Boltzmann distribution:

$$[Ca^{2+}]_0 = [Ca^{2+}]_b \exp\left(\frac{-2e\psi_0}{kT}\right) \quad (1)$$

where the subscript '0' refers to the location of the binding site, subscript 'b' refers to the bulk aqueous solution (far from the membrane), ψ_0 is the electrostatic potential in the aqueous phase at the binding site (relative to that in the bulk solution), e is the magnitude of the electron charge, k is Boltzmann's constant, and T is the absolute temperature *.

$[Ca^{2+}]_0$ is the aqueous Ca^{2+} concentration 'sensed' by the binding site, hence directly determines the amount of Ca^{2+} bound. On the other hand, $[Ca^{2+}]_b$ is the Ca^{2+} concentration that is known experimentally. Therefore, a binding curve plotted as a function of $[Ca^{2+}]_b$ suffers a shift on the $[Ca^{2+}]$ axis as a result of Eqn. 1 if ψ_0 is nonzero. From Eqn. 1, this pCa shift (relative to the case $\psi_0 = 0$) is given by

$$\Delta pCa \equiv pCa_b - pCa_0 = \frac{1}{2.303}\left(\frac{-2e\psi_0}{kT}\right) \quad (2)$$

The electrostatic surface potentials for PC and PS membranes under the present ionic conditions (Fig. 1) can be calculated by use of the Gouy-Chapman-Stern theory. This theory, which combines Gouy-Chapman theory of the diffuse double layer, the Langmuir adsorption isotherm, and the Boltzmann distribution, has been shown to work extremely well for PC and PS membranes in electrolytes similar to those employed here [28,29,35]. For PC membranes the Gouy-Chapman-Stern theory yields an electrostatic surface potential $\psi_0 = +7.0$ mV in 80 mM KCl and 10 mM $MgCl_2$ at 25°C, while for PS membranes the result is $\psi_0 = -29.5$ mV in the same electrolyte. Here we have used the intrinsic association constants $K_I(K:PC) = 0$, $K_I(K:PS) = 0.15\ M^{-1}$, $K_I(Mg:PC) = 2\ M^{-1}$, $K_I(Mg:PS) = 8\ M^{-1}$, competitive binding of K^+ and Mg^{2+} to PS, and phospholipid areas of 70 Å^2 [28,29]. Thus, from Eqn. 2, if the Ca^{2+}-binding site senses ψ_0 at the membrane surface, the expected pCa shift for the PC membrane (relative to a membrane having $\psi_0 = 0$) is $\Delta pCa = -0.24$, while for the PS membrane $\Delta pCa = +1.00$. Therefore the expected pCa shift for the PS membrane relative to the PC membrane is $\Delta pCa = +1.24$ pCa units.

From Fig. 1 it is clear that a pCa shift of such magnitude would lie well outside the experimental scatter of the data. In fact the PS-ATPase and

* In our experiments the aqueous concentration of Ca^{2+} is buffered with EGTA. Since each of the charged states of EGTA and its Ca^{2+} complexes is subject to a Boltzmann relation analogous to Eqn. 1, the Ca^{2+}-buffering reactions are affected by the electrostatic potential. However, from the principle of detailed charge balance and the Boltzmann distribution, it is possible to demonstrate that the equilibria of these reactions are not shifted in the presence of the electrostatic potential and that Eqn. 1 remains valid.

PC-ATPase binding curves appear to be coincident. The binding curve for sarcoplasmic reticulum vesicles, whose phospholipid surface potential (based on sarcoplasmic reticulum lipid composition) should lie between that of the PS and PC membranes, is also virtually the same.

From the above analysis and the data of Fig. 1, we can say conclusively that the ATPase Ca^{2+} binding site does not sense the phospholipid electrostatic surface potential of the membrane. We note that Bell and Miller [30], after incorporating sarcoplasmic reticulum K^+ channels into planar bilayers formed from neutral and from negatively-charged phospholipids, found the channel's K^+ conductance to respond only partially to the membrane electrostatic surface potential, leading to the possibility that the channel's entryway is 10–20 Å away from the membrane surface. Our ATPase Ca^{2+} binding site is even less sensitive to phospholipid surface charge than is the K^+ channel of sarcoplasmic reticulum. This also may be due to location of the binding domain at some distance from the membrane surface so that, as a result of ionic screening, it senses an electrostatic potential of reduced magnitude. Estimates based on Fig. 1 and the Debye screening length predict a binding-site distance greater than 20 Å from the membrane surface, consistent with the known extension of the ATPase some 40 Å from the membrane surface into the aqueous phase [31]. Alternatively, the binding domain may be screened from the phospholipid surface charge by interposition of highly polar regions of the protein itself. Also, the binding domain may be electrostatically insensitive to the surrounding phospholipids due to its local charge environment within the protein. Whether the ATPase Ca^{2+} binding site in fact exists in a region of localized protein charge density can be inferred from the data on Ca^{2+} binding to the sarcoplasmic reticulum ATPase in solutions of different ionic strength and composition.

Effects of electrolytes on calcium binding

We now discuss to what extent the effects of different electrolytes on Ca^{2+} binding (Figs. 2–4) can be attributed to (a) the phospholipid membrane surface potential and (b) localized protein charge densities.

(a) Phospholipid membrane surface potential. The phospholipid composition of rabbit skeletal sarcoplasmic reticulum is approximately 66% PC, 17% phosphatidylethanolamine (PE), 11% phosphatidylinositol (PI), 5% sphingomyelin, 1% PS, and less than 1% cardiolipin [31]. Thus, singly negatively-charged lipids (PI and PS) comprise about 12%, and zwitterionic phospholipids about 88%, of total phospholipids. Calculation of ψ_0 at the membrane surface by use of the Gouy-Chapman-Stern theory requires knowledge of the intrinsic association constants for the binding of all ions of interest both to the charged phospholipids (mainly PI) and to the zwitterionic phospholipids (mainly PC and PE). For the data shown in Figs. 2 and 3, the cations of interest are Mg^{2+}, Ca^{2+}, and K^+. The binding constants of these ions for PC and PE are known [28,29]: $K_1(Mg:PC) = 2\ M^{-1}$, $K_1(Ca:PC) = 3\ M^{-1}$, and $K_1(K:PC) = 0$. The binding properties of these ions to PE are virtually the same as to PC. Since the intrinsic binding constants of these ions to PI are not known, we use, as an approximation, the binding constants for phosphatidylglycerol (PG), a phospholipid whose charge composition is similar to that of PI. The reported intrinsic association constants for PG are [28,32]: $K_1(Mg:PG) = 6.0\ M^{-1}$, $K_1(Ca:PG) = 8.5\ M^{-1}$, and $K_1(K:PG) = 0.15\ M^{-1}$.

In addition to Ca^{2+}, Mg^{2+}, and K^+, the media also contain 20 mM Mops buffer, pH adjusted to 6.8 with Tris. Therefore, these buffers contribute ions to the electrolyte at concentrations $[Mops^-] = [Tris^+] = 5.7$ mM, as calculated from the Henderson-Hasselbalch equation with pK_a of Mops = 7.2 at 25°C. For the electrolyte in which both KCl and $MgCl_2$ are deleted, $Tris^+$ and $Mops^-$ are the major ions in solution *. Whereas $Mops^-$ does not bind to negatively-charged phospholipid membranes, $Tris^+$ does bind to such membranes. In the following discussion, we approximate the binding of $Tris^+$ to PI by $K_1(Tris:PS) = 1.1\ M^{-1}$ [28].

* By an argument similar to that used above for Ca-EGTA buffering, it can be shown that the protonation-deprotonation equilibria for the Mops and Tris buffers are not shifted in the vicinity of a charged membrane, so that simple Boltzmann distributions remain valid, and Gouy-Chapman-Stern theory may be used unaltered.

TABLE II

MEMBRANE SURFACE POTENTIALS DUE TO SARCOPLASMIC RETICULUM PHOSPHOLIPIDS [a], PREDICTED p*Ca* SHIFTS DUE TO THESE SURFACE POTENTIALS [b], AND EXPERIMENTAL p*Ca* SHIFTS [c]

Case No.	Electrolyte [c]	λ_D [d] (A)	ψ_0 [a] (mV)	Δp*Ca*(calc.) [b] relative to $\psi_0 = 0$	Δp*Ca*(calc.) relative to case 1	p$Ca_{\frac{1}{2}}$(expt.) [e]	Δp$Ca_{\frac{1}{2}}$(expt.) relative to case 1
1	80 mM KCl + 10 mM $MgCl_2$	9.2	−8.4	+0.28	–	5.65	–
2	no KCl + 10 mM $MgCl_2$	17.6	−10.0	+0.34	+0.06	5.65	0
3	no KCl + no $MgCl_2$ (5.7 mM Tris-Mops)	40.3	−85.9 [f]	+2.90	+2.62	6.37	+0.72
4	80 mM KCl + no $MgCl_2$	10.8	−37.1	+1.25	+0.97	5.95	+0.30
5	200 mM KCl + no $MgCl_2$	6.8	−24.1	+0.81	+0.53	5.82	+0.17

[a] Calculated by the Gouy-Chapman-Stern theory with the intrinsic association constants described in the text.
[b] Calculated by Eqn. 2.
[c] Cases 1, 2, and 3 refer to Fig. 2; cases 1, 3, 4, and 5 refer to Fig. 3.
[d] Debye screening length of the electrolyte in column 2 at 25°C.
[e] p$Ca_{\frac{1}{2}}$ is the value of p*Ca* at which the ATPase binding site is 50% saturated.
[f] In low ionic strength electrolytes where the added Ca^{2+} is sufficient to alter ψ_0 (i.e., case 3), ψ_0 is given at p*Ca* = p$Ca_{\frac{1}{2}}$.

TABLE III

CALCULATED LOCAL ELECTROSTATIC POTENTIALS AND LOCAL CHARGE DENSITIES AT THE Ca^{2+} BINDING SITE

Case No.	Electrolyte	Δp$Ca_{\frac{1}{2}}$(expt.) relative to case 1 [a]	$\Delta\psi_0$ (mV) relative to case 1 [b]	ψ_0 (mV) at binding site [c]	σ (10^{-4} charge/Å^2) at binding site [d]
1	80 mM KCl + 10 mM $MgCl_2$	–	–	0	0
3	no KCl + no $MgCl_2$ (5.7 mM Tris-Mops) [e]	+0.72	−21.3	−21	−2.4 [f]
4	80 mM KCl + no $MgCl_2$	+0.30	−8.9	−9	−3.6
5	200 mM KCl + no $MgCl_2$	+0.17	−5.0	−5	−3.2

[a] Values taken from Table II.
[b] Calculated by Eqn. 2.
[c] Assuming ψ_0 (case 1) ≈ 0.
[d] Calculated by the Gouy-Chapman theory.
[e] All values for case 3 are at p*Ca* = p$Ca_{\frac{1}{2}}$.
[f] As discussed in the text, the intrinsic charge density here is estimated to be $-3 \cdot 10^{-4}$ charge/Å^2. The indicated value at p*Ca* = p$Ca_{\frac{1}{2}}$ therefore includes $+0.6 \cdot 10^{-4}$ charge/Å^2 due to bound Ca^{2+}.

In Table II we give the results of the Gouy-Chapman-Stern calculations of sarcoplasmic reticulum membrane surface potentials for each case shown in Figs. 2 and 3, based on the sarcoplasmic reticulum phospholipid composition and the intrinsic association constants described above. These values of ψ_0 are those resulting only from the phospholipids and do not include any protein effects. In all cases, ψ_0 of the membrane is perturbed negligibly by calcium ions bound to ATPase. Also, only in case 3 of Table II, i.e. the case $[KCl] = [MgCl_2] = 0$, does the added Ca^{2+} (up to 10^{-4} M) perturb the electrolyte and the surface-charge density of the phospholipids sufficiently to alter ψ_0 of the membrane (see below).

Once ψ_0 has been determined for each electrolyte by use of the Gouy-Chapman-Stern theory (column 4 of Table II), the predicted p*Ca* shift of each ATPase Ca^{2+} binding curve, relative to the case $\psi_0 = 0$, can be calculated by use of Eqn. 2.

These results are shown in column 5 of Table II. In column 6 we list the p*Ca* shift for each electrolyte relative to that of the 'standard' electrolyte, i.e. to case 1. These p*Ca* shifts are those predicted for a Ca^{2+} binding domain fully sensitive to ψ_0 generated by the phospholipids at the sarcoplasmic reticulum membrane surface.

In column 7 of Table II we summarize the experimental $pCa_{1/2}$ values from Figs. 2 and 3. In column 8 we list these values relative to $pCa_{1/2}$ of case 1. We now compare the experimental values of column 8 to the calculated values of column 6.

For case 2, in which KCl is omitted but $MgCl_2$ is retained, no detectable p*Ca* shift is predicted (and none is observed), since the presence of 10 mM $MgCl_2$ is sufficient to 'clamp' the surface potential to a value near −10 mV, irrespective of the presence or absence of 80 mM KCl. Therefore, in order to vary ψ_0, $MgCl_2$ must be deleted and only the monovalent salt varied (Figs. 3 and 4).

In cases 3, 4, and 5, [KCl] is varied from 0 to 80 mM to 200 mM, respectively. Comparison of the predicted p*Ca* shifts (column 6 of Table II) with the observed shifts (column 8), reveals that the latter are uniformly smaller than the former. In fact the observed shifts are consistently about 30% of the shifts predicted on the basis of an ATPase binding site that senses the full surface potential of a sarcoplasmic-reticulum phospholipid membrane. From Eqn. 2 it is seen that the electrostatic p*Ca* shift of a given Ca^{2+} binding curve is directly proportional to the electrostatic potential at the binding site. Therefore, in cases 3–5 the Ca^{2+} binding site must sense an electrostatic potential that is much lower than the potential at the membrane surface.

We can estimate the electrostatic potential at the Ca^{2+}-binding site for cases 3–5 as follows: From Eqn. 2 and the experimental p*Ca* shifts relative to case 1 (column 3 of Table III), ψ_0 at the binding site can be calculated for each case relative to ψ_0 for case 1. These values are shown in column 4 of Table III. Determining the absolute values of ψ_0 for cases 3–5 now requires knowledge of ψ_0 at the binding site for case 1. This value is likely to be very small, since case 1 involves the presence of 10 mM $MgCl_2$. If we assume that $\psi_0 \approx 0$ for case 1, then the values of ψ_0 for cases 3–5 are those listed in column 5 of Table III. It should be noted that these values of ψ_0 at the binding site are all 20–25% of the respective values of ψ_0 at the membrane surface (column 4 of Table II).

The fact that ψ_0 at the binding site is a fraction of ψ_0 at the membrane surface suggests that the binding site may be located some distance from the surface, and hence screened from it by the electrolyte. If so, then the distance necessary to reduce ψ_0 to 20%–25% of its surface value is 1.4–1.6 λ_D, where λ_D is the Debye screening length *. However, from Table II, it is seen that λ_D varies considerably from case 3 to case 5; hence this interpretation requires that the binding-site position change with [KCl], its distance from the surface being 56 Å, 15 Å, and 11 Å, respectively, for cases 3, 4, and 5. Although not impossible, such behavior does not seem likely.

The near constancy of the ratio of ψ_0 at the binding site to ψ_0 at the membrane surface, despite a 35-fold change of electrolyte ionic strength, suggests that electrolyte screening of membrane surface charge does not play an important role in determining ψ_0 at the binding site. This is consistent with the conclusions drawn from the PC-ATPase and PS-ATPase binding data, which indicated that the Ca^{2+} binding site does not sense the phospholipid surface charge of the membrane appreciably.

(b) Localized charge density. An alternative explanation is that ψ_0 is determined by a localized charge density in the protein, situated near the binding site. The effective localized charge density (σ), for each case, can be calculated from the values of ψ_0 in Table III by use of the Gouy-Chapman theory. The results are shown in column 6 of Table III. The values of σ for cases 3–5 range from $-2.4 \cdot 10^{-4}$ to $-3.6 \cdot 10^{-4}$ charge/Å^2, which is significantly less than the intrinsic charge den-

* The Debye screening length is given by

$$\lambda_D = \left\{ \left(\frac{8\pi N_A e^2}{1000 \epsilon k T} \right) I \right\}^{-1/2}$$

where N_A is Avogadro's number, e is the electron charge, ϵ is the dielectric constant of the electrolyte, k is Boltzmann's constant, T is the absolute temperature, and I is the electrolyte ionic strength [33].

sity of the sarcoplasmic reticulum phospholipid membrane, $-17 \cdot 10^{-4}$ charge/Å^2. The reduction of $|\sigma|$ for case 3, compared to case 4, will be discussed in the following section. The small reduction of $|\sigma|$ for 200 mM KCl compared to 80 mM KCl may reflect the existence of some K^+ binding to the protein in the region of the Ca^{2+} binding site.

In Fig. 4, the experimental p*Ca* shifts for these monovalent-cation chloride salts occur in the order $Cs^+ \gtrsim$ choline$^+ > K^+ > Li^+$. In terms of the protein local charge density, these data imply that the monovalent cations must bind in this local region. Since the electrolyte ionic strengths, and hence the Debye screening lengths, are the same for all four electrolytes, the intrinsic protein charge density should not change (as a result of altered screening between protein charges and altered charge-charge repulsions) from one electrolyte to the other. The different p*Ca* shifts in Fig. 4, which reflect different values of ψ_0 at the binding site and different values of localized charge density, must therefore result from different amounts of monovalent cation bound. (It was mentioned above that the data of Fig. 3 also suggest K^+ binding.) Moreover, the fact that at saturating Ca^{2+} the maximal amount of Ca^{2+} bound is independent of the electrolyte suggests that monovalent-cation vs. Ca^{2+} binding is of a competitive nature.

It is clear from Fig. 4 that the relative binding strengths of the monovalent cations to the protein in the vicinity of the Ca^{2+} binding site occur in the sequence $Li^+ > K^+ >$ choline$^+ \gtrsim Cs^+$. This order is the same as the order of binding strengths of these ions to PS and PG membranes (except perhaps for choline, which has not been reported) [28].

Effect of electrostatic potential on cooperativity of Ca^{2+} binding

All but one of the Ca^{2+} binding curves of Figs. 1–4 display cooperative behavior, having Hill coefficients near 2 [2]. However, the curve measured under low ionic strength conditions shows an apparent reduction of cooperativity. We now consider whether such behavior can be attributed to electrostatic effects.

In the Ca^{2+} binding experiments, free aqueous $[Ca^{2+}]$ is varied from 10^{-7} M to $3 \cdot 10^{-5}$ M. For the moderate and high ionic-strength electrolytes, such small additions of Ca^{2+} are not sufficient to alter ψ_0 at the binding site. In effect, ψ_0 is 'clamped' by the electrolyte irrespective of the value of p*Ca*. The result, as seen from Eqns. 1 and 2, is that the Ca^{2+} binding curves are simply shifted on the p*Ca* axis with no change of shape. However, for case 3 of Figs. 2 and 3, where the ionic strength is only 5.7 mM, the Ca^{2+} additions apparently are able to alter ψ_0. The result is as follows: As $[Ca^{2+}]$ increases, ψ_0 becomes less negative due to screening and binding of Ca^{2+} to the protein or membrane. The lowered $|\psi_0|$ causes less p*Ca* shift (relative to the case $\psi_0 = 0$) than would otherwise occur. Since $|\psi_0|$ decreases as p*Ca* decreases, the binding curve becomes distorted, splaying to the right at low p*Ca*. This effect is clearly seen for case 3 of Fig. 2, where little distortion is evident in the lower part of the curve ($pCa > pCa_{1/2}$), while the upper part of the curve ($pCa < pCa_{1/2}$) is skewed to the right. This type of distortion is most suggestive of electrostatic effects. It gives the appearance of a binding cooperativity that decreases as a function of decreasing p*Ca*.

To gain more insight into this phenomenon, we have used the Gouy-Chapman-Stern theory to calculate the distortion of the binding curve expected on the basis of simple electrostatics. The magnitude of the distortion is quantified using Fig. 2 as follows: At 10% of saturation, p*Ca* of the distorted curve (i.e., left-hand curve) is 6.90, compared to 6.10 of the reference curve (right-hand curve). Therefore, the difference or p*Ca* shift of the distorted curve relative to the reference curve at 10% of saturation is $\Delta pCa^{10} = 0.80$ p*Ca* units. Similarly, at 50% of saturation we find $\Delta pCa^{50} = 0.72$ units, and at 90% of saturation $\Delta pCa^{90} = 0.40$ units. From Eqn. 2, the difference between ψ_0 of the shifted curve and ψ_0 of the reference curve at each level of saturation can be determined: $\Delta\psi_0^{10} = -23.7$ mV, $\Delta\psi_0^{50} = -21.3$ mV, $\Delta\psi_0^{90} = -11.8$ mV. (Note that $\Delta\psi_0^{50}$ here agrees with the same quantity in Table III.) If we assume that ψ_0 of the reference curve is independent of p*Ca* in this range, as indicated by the symmetry of this curve, then ψ_0 of the distorted curve increases by 2.4 mV between 10% and 50% of saturation, and it increases by 9.5 mV between 50%and 90% of saturation.

Using the local charge density previously determined for case 3 at $pCa_{1/2}$ (cf. Table III), we can calculate with the Gouy-Chapman-Stern theory the expected change of ψ_0 as p*Ca* ranges from 6.9 (10% of saturation) to 5.5 (90% of saturation) in case 3. If Ca^{2+} only screens and does not bind, the predicted change of ψ_0 over the above p*Ca* range is insignificant (< 0.1 mV). Alternatively, if we assume, as a result of the low ionic strength and large λ_D of this electrolyte, that ψ_0 at the binding site is affected by changes of the phospholipid surface potential of the membrane, and that Ca^{2+} binds to the phospholipids as previously described, again the predicted change of ψ_0 at the binding site over the relevant p*Ca* range is far too small (1.2 mV) to produce the observed effects. In fact, for $\psi_0 \approx -20$ mV, a change of 11.9 mV over a p*Ca* range of 6.9 to 5.5 is a very large change indeed. It can only be produced from the Gouy-Chapman-Stern theory if Ca^{2+} binds to the protein in the localized charge region, thus effecting a change of the localized charge density. If Ca^{2+} is assumed to bind to the negatively-charged groups that comprise the localized charge density, then an intrinsic localized charge density of $-3 \cdot 10^{-4}$ charge/Å^2 and an intrinsic association constant of $5 \cdot 10^4$ M^{-1} produce an excellent fit to (a) the correct ψ_0 and charge density at $pCa_{1/2}$ (cf. Table III) and (b) the correct changes of ψ_0 (i.e., distortion of the binding curve) over the entire relevant p*Ca* range. The Gouy-Chapman-Stern theoretical curve calculated with the above parameters is shown by the dashed curve in Fig. 2.

It is important to realize that the calculated curve in Fig. 2 is generated by the Gouy-Chapman-Stern theory with only two fitted parameters: the intrinsic protein localized charge density and the intrinsic Ca^{2+} association constant described above. In this treatment, the distortion ('loss of cooperativity') of the binding curve at low ionic strength occurs as the result of a progressive p*Ca* shift relative to the 'standard' binding curve at high ionic strength. This kind of shift, in turn, arises from the fact that at low ionic strength ψ_0 is Ca^{2+}-dependent, i.e., ψ_0 is progressively altered by Ca^{2+} binding to a localized charge density in the protein.

Both theoretical and experimental limitations preclude a precise description of the localized protein charge. Neither the Gouy-Chapman-Stern theory, which treats charged domains in terms of a mean charge density, nor currently-available structural information of the ATPase, provides grounds for elucidating the source of this charge. It could result from charged residues in the vicinity of the Ca^{2+}-binding domains or, alternatively, the charge may be intrinsic to the Ca^{2+}-binding domains themselves. If the latter is the case, then the distortion of the binding curve at low ionic strength might result from the high-affinity Ca^{2+} binding itself, with each bound Ca^{2+} altering ψ_0 and electrostatically repelling other calcium ions from neighboring binding domains. Thus, an anti-cooperative electrostatic effect becomes superimposed on the intrinsic cooperative mechanism of the protein. This scheme requires that the Ca^{2+}-binding domains of neighboring polypeptide chains lie approximately within a Debye screening length of one another (40 Å in the present case).

In conclusion, we attribute the distortion of calcium binding isotherms in low ionic-strength media to discrete electrostatic phenomena in the protein binding domains. The only arbitrary assumption in the above discussion is that $\psi_0 \approx 0$ at the Ca^{2+}-binding domain for the 80 mM KCl + 10 mM $MgCl_2$ electrolyte. If this assumption is inaccurate, the numerical details of the above arguments will differ, but the general principles will remain the same.

Acknowledgements

We thank Dr. Alexander Murphy for helpful discussions. This research was supported by grants from the National Institutes of Health (HL-27867) and the Muscular Dystrophy Association. Dr. H. Scofano was supported by a Fogarty International Fellowship.

References

1 Chevalier, J. and Butow, R.A. (1971) Biochemistry 10, 2733–2737
2 Inesi, G., Kurzmack, M., Coan, C. and Lewis, D.E. (1980) J. Biol. Chem. 255, 3025–3031
3 Verjovski-Almeida, S. and Silva, J. (1981) J. Biol. Chem. 256, 2940–2944
4 Hill, T.L. and Inesi, G. (1982) Proc. Natl. Acad. Sci. USA 79, 3978–3982

5 Watanabe, T., Lewis, D., Nakamoto, R., Kurzmack, M., Fronticelli, C. and Inesi, G. (1981) Biochemistry 20, 6617–6625
6 MacLennan, D.H. (1970) J. Biol. Chem. 249, 980–984
7 Meissner, G., Conner, G.E. and Fleischer, S. (1973) Biochim. Biophys. Acta 298, 246–269
8 Barrabin, H., Scofano, H. and Inesi, G. (1984) Biochemistry 23, 1542–1548
9 Gafni, A. and Boyer, P.D. (1984) Biochemistry 23, 4362–4367
10 Coll, R. and Murphy, A.J. (1984) J. Biol. Chem. 259, 14249–14254
11 Eletr, S. and Inesi, G. (1972) Biochim. Biophys. Acta 282, 174–179
12 Lin, T. and Morales, M. (1977) Anal. Biochem. 77, 10–17
13 Fernandez-Belda, F., Kurzmack, M. and Inesi, G. (1984) J. Biol. Chem. 259, 9687–9698
14 Dupont, Y. (1976) Biochem. Biophys. Res. Commun. 71, 544–550
15 Guillain, F., Champeil, P., Lacapere, J. and Gingold, M. (1981) J. Biol. Chem. 256, 6140–6147
16 Fabiato, A. and Fabiato, F. (1979) J. Physiol. (Paris) 75, 463–505
17 Allen, D.G., Blinks, J.R. and Prendergast, F.G. (1977) Science 196, 996–998
18 Lowry, O.H., Rosebrough, N.J., Farr, A.L. and Randall, R.J. (1951) J. Biol. Chem. 193, 265–275
19 Peterson, G.L. (1977) Anal. Biochem. 83, 346–356
20 Barlett, G.R. (1959) J. Biol. Chem. 234, 466–468
21 Fiehn, W. and Migala, A. (1971) Eur. J. Biochem. 20, 245–248
22 Medda, P. and Hasselbach, W. (1985) Eur. J. Biochem. 146, 255–260
23 Hasselbach, W. (1964) Prog. Biophys. Mol. Biol. 14, 167–222
24 Dean, W. and Tanford, C. (1978) Biochemistry 17, 1683–1690
25 Kosk-Kosicka, D., Kurzmack, M. and Inesi, G. (1983) Biochemistry 22, 2559–2567
26 Ikemoto, N., Garcia, A., Kurobe, Y. and Scott, T. (1981) J. Biol. Chem. 256, 8593–8601
27 Taylor, K.A., Dux, L. and Martonosi, A. (1984) J. Mol. Biol. 174, 193–204
28 Eisenberg, M., Gresalfi, T., Riccio, T. and McLaughlin, S. (1979) Biochemistry 18, 5213–5223
29 McLaughlin, S., Mulrine, N., Gresalfi, T., Vaio, G. and McLaughlin, A. (1981) J. Gen. Physiol. 77, 445–473
30 Bell, J.E. and Miller, C. (1984) Biophys. J. 45, 279–287
31 Martonosi, A.N. and Beeler, T.J. (1983) in Handbook of Physiology, Section 10: Skeletal Muscle (Peachey, L.D., Adrian, R.H. and Geiger, S.R., eds.), pp. 417–485, Am. Physiol. Soc., Bethesda, MD
32 Lau, A., McLaughlin, A. and McLaughlin, S. (1981) Biochim. Biophys. Acta 645, 279–292
33 Bockris, J.O'M. and Reddy, A.K.N. (1973) Modern Electrochemistry, p. 210, Plenum/Rosetta, New York
34 Highsmith, S.R. (1982) Biochemistry 21, 3786–3789
35 Cohen, J.A. and Cohen, M. (1981) Biophys. J. 36, 623–651